

Support and solvent effects on the liquid-phase chemoselective hydrogenation of crotonaldehyde over Pt catalysts

Jesús Hidalgo-Carrillo, María Angeles Aramendía, Alberto Marinas, José María Marinas, Francisco José Urbano*

Department of Organic Chemistry, University of Córdoba, Campus de Rabanales, Edificio C-3, Ctra Nnal IV, km 396, 14014 Córdoba, Spain

ARTICLE INFO

Article history:

Received 11 May 2010

Received in revised form 16 June 2010

Accepted 6 July 2010

Available online 13 July 2010

Keywords:

Pt catalyst

Chemoselective crotonaldehyde hydrogenation

Crotyl alcohol selectivity

Solvent effect

Catalyst reduction temperature effect

ABSTRACT

A study of the selective reduction of crotonaldehyde to crotyl alcohol over Pt catalysts supported on various partially reducible solids including Fe_2O_3 , Fe_3O_4 , ZrO_2 , ZnO , TiO_2 and SnO_2 was conducted. The catalysts were characterized by thermal programmed reduction (TPR) and reduced at temperatures that were selected as a function of the presence of specific reduction peaks for Pt in the TPR profiles. The reduced catalysts were studied by XRD spectroscopy and TEM, and used for the liquid-phase hydrogenation of crotonaldehyde. As a rule, low reduction temperatures led to catalysts providing high yields in the unsaturated alcohol (2-butenol). Such yields were substantially increased by the addition of water in mixtures with dioxane to the medium, whether the medium was acid, neutral or basic. The highest selectivity towards crotyl alcohol was obtained with the solid Pt/ZnO reduced at 175 °C. This may have resulted from the presence of ZnO_xCl_y species forming around Pt particles, which were detected by XPS and might have acted as Lewis acid sites facilitating anchoring of crotonaldehyde via its carbonyl double bond. The optimum working conditions, which included a reaction temperature of 30 °C and an initial hydrogen pressure of 0.414 MPa, afforded a selectivity higher than 90% for crotyl alcohol at conversions in the region of 40%.

© 2010 Elsevier B.V. All rights reserved.

1. Introduction

The selective hydrogenation of unsaturated aldehydes to unsaturated alcohols over heterogeneous catalysts has aroused considerable attention as a result of its usefulness for the flavor, fragrance and pharmaceutical industries [1]. The most challenging class of these chemoselective hydrogenation reactions is the reduction of α,β -unsaturated aldehydes to allyl alcohols. This chemoselective hydrogenation of carbonyl compounds over heterogeneous catalysts has been recently reviewed [2]. The activity and unsaturated alcohol selectivity of unpromoted catalysts is dependent on the particular type of metal they contain. Unpromoted Ir and Os catalysts are known to be highly selective, those of Ru and Co moderately selective, and those of Pd, Rh and Ni unselective towards the formation of the unsaturated alcohol [3].

The performance of unpromoted catalysts can be improved by using an appropriate promoter. Thus, ionic metal promoters increase alcohol selectivity by coordinating with and polarizing the aldehyde group, thereby enhancing its activity [4]. Recently, the addition of Zn and/or Fe to a Pt catalyst was found to have a

substantial promoting effect on its activity and alcohol selectivity in the hydrogenation of cinnamaldehyde; the effect was ascribed to electron transfer from Zn and Fe to Pt particles (reflected in XPS analyses) and the formation of electrophilic sites for the carbonyl group to anchor [5]. Also, the electron density of the catalytic metal was found to be increased by the effect of its alloying with a more electropositive metal [6,7] or the use of an electron-rich support [8,9]. Thus, gold supported on various oxides considerably altered the selectivity towards hydrogenation of the conjugated C=O bond in benzalacetone [10], which was highly correlated with the reducibility of the support. Their correlation was ascribed to electron transfer from the reduced support to the metal leading to the formation of electron-enriched gold particles facilitating C=O hydrogenation on their surface [10]. Other reducible oxides in addition to those of iron have been found to contribute to changes in catalytic activity and selectivity in the hydrogenation of unsaturated carbonyl compounds over Pt catalysts; such oxides include TiO_2 [11], SnO_2 [12], Nb_2O_5 [13], Y_2O_3 [14], ZrO_2 [15], ZnO [16] and CeO_2 [17].

The selective hydrogenation of crotonaldehyde over Pt supported catalysts can be used as a probe reaction sensitive to metal-support interactions [18–20]. In other words, when the metal is not modified by the support, the C=C bond is selectively hydrogenated; otherwise, the carbonyl bond is the selective target

* Corresponding author. Tel.: +34 957218638; fax: +34 957212066.
E-mail address: FJ.Urbano@uco.es (F.J. Urbano).

with the metal in an SMSI state. However, the origin of the specific behavior of Pt in such a state remains a controversial subject for some supports. Thus, the SMSI effect on the selective reduction of the C=O bond in α,β -unsaturated carbonyl compounds might be related to (a) the formation of an alloy between Pt and the reduced metal in the support [18]; (b) an electronic effect of Pt particles due to partial reduction of the support [21]; or (c) the decoration of Pt particles with patches of partially reduced support [17].

In addition to the active metal, the activity and selectivity for the reduction of the C=O bond in unsaturated carbonyl compounds is influenced by additional factors including the metal precursor [12,16], solvent [2,22–25], metal particle size [2,26], synthetic procedure for the catalytic system [23,26], use of additives [27], various reaction conditions such as temperature and hydrogen pressure, and whether the process is conducted in the gas or liquid-phase [26]. Additionally, the change in metal particle size can affect the electronic and geometrical properties of the metal particles. The smaller metal particles are known to be more electron deficient than larger ones. Furthermore, the number of edges and corners, which could have different activities and selectivities is increased in the smaller particles [2].

Singh and Vannice reviewed the solvent effects on heterogeneously catalysed reactions [23]. The most salient effects on the hydrogenation of α,β -unsaturated aldehydes are solvent polarity, hydrogen solubility, catalyst–solvent interactions and reactant solvation in the bulk liquid-phase. Although rationalizing solvent effects is very difficult owing to the lack of systematic experimental data, recent trends regarding solvent polarity suggest that polar solvents boost the hydrogenation of C=O bonds and raise the selectivity towards the unsaturated alcohol whereas non-polar solvents favor hydrogenation of the non-polar C=C bond [2,28,29]. Also, the addition of water has been found to increase the selectivity for the unsaturated alcohol in both Pd/C and Pt/C catalysts [29]. Some authors have noted that the hydrophilic nature of the C=O bond facilitates its selective hydrogenation in pure water [22] and water/organic solvent mixtures [30].

Most of the papers published on the Pt catalysed selective hydrogenation of crotonaldehyde deal with gas-phase reactions. In this sense, recently, Rynkowski et al. [31] summarized the activity and selectivity obtained for different Pt/support catalysts in selective hydrogenation of crotonaldehyde in the gas phase. However, as far as liquid-phase selective hydrogenation of crotonaldehyde over Pt catalysts is concerned, the published works are relatively scarce. Bartok et al. reported the activity and selectivity for several Pt/support catalysts in the liquid-phase providing TOF (s^{-1}) values in the 10^{-1} to 10^{-2} range with selectivities to crotyl alcohol between 7 and 43% [28].

In this work, we explored the liquid-phase Pt-catalysed selective hydrogenation of crotonaldehyde as a test reaction for analysing the effect of various reducible supports including Fe_2O_3 , Fe_3O_4 , ZrO_2 , TiO_2 , ZnO and SnO_2 , and examining the solvent effect on activity and selectivity towards the unsaturated alcohol.

2. Experimental

2.1. Synthesis of Pt supported catalysts

The catalysts studied were obtained from an aqueous solution containing 8% (w/w) chloroplatinic acid (Sigma–Aldrich Ref. 262587) as metal precursor and the following metal oxides as supports: tin (IV) oxide (Sigma–Aldrich Ref. 549657), zirconium (IV) oxide (Sigma–Aldrich Ref. 544760), zinc (II) oxide (Sigma–Aldrich Ref. 544906), iron (II,III) oxide (Sigma–Aldrich Ref. 637106), iron (III) oxide (Sigma–Aldrich Ref. 544884) and titanium (IV) oxide (Degussa, P-25).

The synthetic procedure was as follows: a volume of 6.57 mL of chloroplatinic acid solution was diluted to 200 mL with Milli-Q water and adjusted to pH 7 by adding 0.1 M NaOH (FLUKA Ref. 43617). Then, an amount of 4.75 g of support was added and the mixture readjusted to pH 7 with NaOH for acid supports or HCl for basic supports. The solution containing the support was refluxed at 80 °C under vigorous stirring for 2 h. Then, a volume of 10 mL of isopropanol was added, the temperature raised to 110 °C and refluxing continued for 30 min, after which the mixture was vacuum filtered and the filtrate washed with three portions of 25 mL of water each. The resulting solid was dried in a muffle furnace at 110 °C for 12 h, ground and calcined at 400 °C for 4 h. After calcination, the solid was ground again, sieved through a mesh of 0.149 mm pore size and stored in a topaz flask. The nominal proportion of Pt in the catalyst thus obtained was 5 wt%. Finally, the catalyst was reduced under a hydrogen stream flowing at 30 mL/min at selected temperatures for 2 h. Reduction temperature was chosen according to significant features observed in the temperature-programmed reduction profiles. The solid names used included the metal, its support and the reduction temperature used (e.g. Pt/ZnO-175).

2.1.1. Characterization of catalysts

The textural properties of the solids calcined at 400 °C (viz. specific surface area, pore volume and mean pore radius) were determined from nitrogen adsorption–desorption isotherms obtained at liquid nitrogen temperature on a Micromeritics ASAP-2010 instrument. Surface areas were calculated with the Brunauer–Emmett–Teller (BET) method. All samples were degassed to 0.1 Pa at 110 °C prior to measurement.

Elemental analysis of Pt containing samples was performed by the staff at the Central Service for Research Support (SCAI) of the University of Córdoba, using inductively coupled plasma mass spectrometry (ICP-MS). Measurements were made on a Perkin–Elmer ELAN DRC-e instrument following dissolution of the sample in a 1:1:1 $H_2SO_4/HF/H_2O$ mixture. Calibration was done by using PE Pure Plus atomic spectroscopy standards, also from Perkin–Elmer.

Transmission electron microscopy (TEM) images were obtained at the SCAI of the University of Córdoba by using a Philips CM-10 microscope for low magnification samples and a JEOL JEM 2010 microscope for high magnification samples. All samples were mounted on 3 mm holey carbon copper grids.

EDX measurements were made with a JEOL JSM-6300 scanning electron microscope (SEM) equipped with an energy-dispersive X-ray (EDX) detector.

X-ray patterns for the samples were obtained with a Siemens D-5000 diffractometer equipped with a DACO-MP automatic control and data acquisition system. The instrument was used with CoK_{α} radiation and a graphite monochromator.

Temperature-programmed reduction (TPR) measurements were made with a Micromeritics TPD-TPR 2900 analyser. An amount of 200 mg of catalyst was placed in the sample holder and reduced in a 5:95 H_2/Ar stream flowing at 40 mL/min. The temperature was ramped from 0 to 850 °C at $10^{\circ}C\ min^{-1}$; by exception, the upper limit for solids Pt/ZnO and Pt/ SnO_2 was 500 °C.

X-ray photoelectron spectroscopy (XPS) data were recorded on 4 mm \times 4 mm pellets 0.5 mm thick that were obtained by gently pressing the powdered materials following outgassing to a pressure below about 2×10^{-8} Torr at 150 °C in the instrument pre-chamber to remove chemisorbed volatile species. The main chamber of the Leibold-Heraeus LHS10 spectrometer used, capable of operating down to less than 2×10^{-9} Torr, was equipped with an EA-200 MCD hemispherical electron analyser with a dual X-ray source using AlK_{α} ($h\nu = 1486.6\ eV$) at 120 W, at 30 mA, with C(1s) as energy reference (284.6 eV).

Table 1
Specific surface area (S_{BET}) and chemical composition obtained by ICP-PS and SEM-EDX for the catalysts synthesized.

Catalyst	S_{BET} ($\text{m}^2 \text{g}^{-1}$)	%Pt, w/w Theoretical	%Pt, w/w ICP-MS	%Pt, w/w EDX
Pt/Fe ₂ O ₃	19	5	5.6	2.9
Pt/Fe ₃ O ₄	40	5	6.1	3.6
Pt/ZrO ₂	42	5	6.4	3.6
Pt/ZnO	18	5	5.1	3.7
Pt/TiO ₂	52	5	4.5	0.7
Pt/SnO ₂	18	5	–	1.6

2.2. Liquid-phase hydrogenation of crotonaldehyde

The liquid-phase hydrogenation of crotonaldehyde with molecular hydrogen was conducted on a Parr Instruments 3911 low-pressure reactor, using a constant rate of 300 shakes min^{-1} . The reaction vessel (500 mL in volume) was wrapped in a metal jacket through which thermostated water was circulated. The apparatus was equipped with a gauge that recorded the pressure inside the reaction vessel throughout the experiment. All reactions were performed with an overall liquid volume of 20 mL containing 0.5 M crotonaldehyde in the selected solvent, using an initial pressure of 0.414 MPa and a temperature of 30 °C. Prior to each run, an amount of 100 mg of calcined Pt catalyst was reduced in a hydrogen stream flowing at 30 mL/min at the selected temperature for 2 h and then cooled in the same stream. The standard operational procedure used in each experiment was as follows: the reaction vessel was loaded with 20 mL of 0.5 M crotonaldehyde, sonicated for 15 min and 100 mg of freshly reduced catalyst were added. The reaction vessel was then attached to the reactor and, once the temperature levelled off at 30 °C – which took about 10 min –, the vessel was evacuated and filled with hydrogen to a pressure of 0.414 MPa twice. After 15 min, the pressure was readjusted, the shaking device started and the reaction timed. Blank tests intended to ascertain that no reaction would take place thermally in the absence of catalyst were conducted with a reaction mixture consisting solely of substrate and solvent. No signs of reaction were detected after 8 h under these conditions.

Reaction products were analysed on a Fisons gas chromatograph equipped with a flame ionization detector (FID) and a Supelcowax-10 column (30 m long \times 0.25 mm ID, 0.25 μm film thickness). A calibration plot for each product was constructed from commercially available standards. The products of the reduction of crotonaldehyde (designated “unsaturated aldehyde”, UAL) were crotyl alcohol (“unsaturated alcohol”, UOL), 1-butanol (“saturated alcohol”, SOL) and butanal (“saturated aldehyde”, SAL). Crotonaldehyde conversion (X_{UAL}) was calculated as $(C_{\text{UAL}}^0 - C_{\text{UAL}})/C_{\text{UAL}}^0$, where C_{UAL}^0 is the initial concentration of crotonaldehyde and C_{UAL} that at reaction time t . The selectivity of each reaction product was calculated as $\% \text{Sel}_i = C_i / \sum C_i \times 100$.

3. Results and discussion

3.1. Characterization of catalysts

3.1.1. Surface area and chemical composition

Table 1 shows the chemical composition and surface area of the catalysts. Chemical composition data were obtained by ICP-MS analysis and microchemical data by energy-dispersive X-ray analysis (SEM-EDX). Based on the ICP-MS results, Pt was highly efficiently or even virtually completely incorporated onto all supports; the EDX values, however, were roughly one-half the ICP-MS values. This suggests that some Pt species migrate into the catalyst particles or that, following reduction, the partially reducible supports coat or decorate Pt particles and render them less “visible”

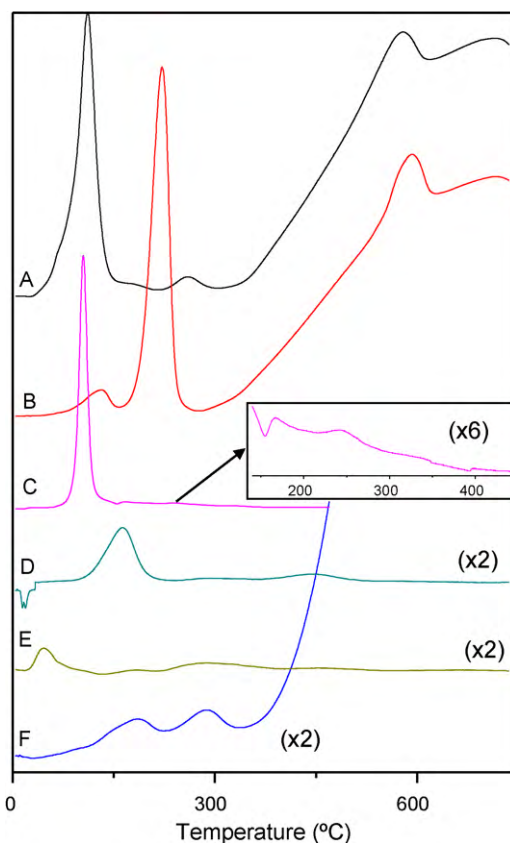


Fig. 1. Temperature-programmed reduction (TPR) profiles obtained for the catalyst synthesized in this work: (A) Pt/Fe₃O₄; (B) Pt/Fe₂O₃; (C) Pt/ZnO (D) Pt/ZrO₂; (E) Pt/TiO₂; (F) Pt/SnO₂.

to the EDX technique—which has an analysis depth capacity less than 2 μm . The EDX determined Pt surface content of solid Pt/TiO₂ was especially low (0.7%), even if one considers that this was the catalyst containing the lowest total proportion of Pt (4.5%).

3.1.2. Temperature-programmed reduction

The TPR profiles differed markedly from one another by effect of the marked differences in redox properties between the catalysts. In some cases, the support was hardly reducible; in others, it exhibited several reduction peaks at different temperatures. In any case, identifying the reduction peaks for Pt and the support facilitated selection of the most suitable reduction temperature for each catalyst with a view to its use in the liquid-phase hydrogenation of crotonaldehyde.

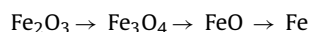
Fig. 1 shows the TPR profiles for the solids calcined at 400 °C. As can be seen, the profile for Pt/ZrO₂ exhibited a reduction peak at 181 °C that was assigned to the reduction of oxidized platinum species to metallic Pt [32]. Also, it contained two weaker reduction peaks at 317 and 477 °C which, based on the low reducibility of the ZrO₂ support, were assigned to the reduction of Pt species strongly interacting with it [32] or the partial, Pt-catalysed reduction of the support via spillover of hydrogen from the metal to the ZrO₂ [32–34]. Platinum and zirconium oxide were previously found to exhibit strong metal–support interactions, albeit in solids reduced at temperatures above 400 °C [32]. Such interactions diminish the hydrogen adsorption capacity of the reduced catalyst.

The TPR profile for solid Pt/ZnO was finished below 500 °C, where Zn sublimates under reductive conditions. In catalysts prepared from chloroplatinic acid, this solid exhibits a strong reduction peak at 250–300 °C [16] which has been ascribed to the reduction of oxychloride species of the $[\text{Pt}(\text{OH})_4\text{Cl}_2]^{2-}$ type formed by calcina-

tion of the platinum precursor H_2PtCl_6 [16,35]. The reduction takes 3 mol of H_2 per mol of Pt precursor—hence the strength of the TPR peak observed. Our TPR profile exhibited a strong reduction peak at 110°C in addition to two much weaker peaks at 178 and 285°C . The reduction temperature for the first peak, 110°C , was markedly low relative to previously reported values for the reduction of oxychloride Pt species ($250\text{--}300^\circ\text{C}$). However, our catalysts were prepared in such a way that the addition of 2-propanol to the catalyst mixture at the end of the synthetic process may have caused the partial reduction of chloroplatinic acid, as detected from the loss of the yellowish color of its solution. This probably precludes the formation of the above-mentioned oxychloride species after calcination [16]. A more plausible explanation in our case is that, upon calcination of the catalyst, the platinum may be present as metal Pt or, more probably, as Pt^0 coated particles of PtO or PtO_2 . In this situation, the catalyst may behave like those prepared from chloride-free precursors such as $\text{Pt}(\text{NH}_3)_4(\text{NO}_3)_2$, calcination of which provides metal Pt particles coated with PtO that are reduced at a lower temperature ($120\text{--}160^\circ\text{C}$) [16,35]. As a result, the solid must have been reduced at lower temperatures, as seen in our TPR profile. The small reduction peaks observed at higher temperatures can be assigned to the reduction of ZnO to metal Zn, which may alloy with Pt [16]. The XRD technique provided additional confirmation.

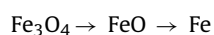
The TPR profile for solid Pt/SnO_2 was also stopped at 500°C —like Zn in ZnO , Sn sublimates above this temperature in a reductive environment. The profile exhibited two reduction peaks at low temperatures (192 and 297°C) in addition to a strong, truncated peak near 500°C . The latter was assigned to the reduction of SnO_2 to Sn^0 [34,36] and the former two to that of PtO_x species interacting to a variable extent with the support [34].

The TPR profile for $\text{Pt}/\text{Fe}_2\text{O}_3$ exhibited three distinct regions. The first contained a small peak at a low temperature (130°C); the second a sharp, strong peak at 223°C ; and the third a complex, broad signal not shown in the graph which contained two ill-defined peaks at 605 and 737°C . The last region involved much higher adsorption of hydrogen than the previous two. All this suggests that the peak at 130°C was due to the reduction of Pt oxidized species to Pt^0 . Also, based on previously reported data for Fe_2O_3 , the sharp peak at 223°C , and the broad signal with two maxima at 605 and 737°C , can be assigned to reduction of the support [37–39]. According to Munteanu et al. [39], the reduction of Fe_2O_3 involves the following three steps:



These three steps reflect as a strong, variably sharp peak at a low temperature (ca. 400°C) and a broader, occasionally shouldered peak at higher levels ($500\text{--}800^\circ\text{C}$) in the TPR profiles. This is quite consistent with our profiles, the sole appreciable difference being the temperature for the second, sharp, strong peak, which was markedly lower than its reported values. However, the presence of a metal such as Au on a Fe_2O_3 support has also been found to lower the temperature for the first reduction peak (that for the $\text{Fe}_2\text{O}_3 \rightarrow \text{Fe}_3\text{O}_4$ transition) through a catalytic effect of the metal on the reduction of Fe_2O_3 [38,39]. Therefore, the presence of Pt on Fe_2O_3 might have facilitated the reduction of Fe_2O_3 to Fe_3O_4 to an extent causing the associated peak to appear at such a low temperature as 223°C .

The profile for solid $\text{Pt}/\text{Fe}_3\text{O}_4$ was quite similar to that for $\text{Pt}/\text{Fe}_2\text{O}_3$. It contained a strong reduction peak at a low temperature (116°C) and two smaller ones at 184 and 271°C in addition to a broad band with two maxima at 596 and 736°C echoing that for $\text{Pt}/\text{Fe}_2\text{O}_3$. Based on the previous argument, such a band can be assigned to the reduction of the oxide to metal Fe in two steps:

**Table 2**

Influence of the catalyst reduction temperature on the activity (crotonaldehyde conversion, X_{UAL}) and selectivity to butanal (S_{SAL}), 1-butanol (S_{SOL}) and crotyl alcohol (S_{UOL}) obtained in the liquid-phase crotonaldehyde hydrogenation.

Catalyst	Reduction temperature ($^\circ\text{C}$)	X_{UAL} (%)	S_{SAL} (%)	S_{SOL} (%)	S_{UOL} (%)
Pt/ZrO ₂	400	50	76	23	2
	317	13	83	12	6
	180	37	82	14	4
Pt/ZnO	400	1	68	9	23
	175	1	25	0	75
Pt/SnO ₂	400	3	89	7	4
	290	1	75	0	25
	190	<1	46	16	38
Pt/Fe ₂ O ₃	400	2	58	17	25
	130	20	56	29	15
Pt/Fe ₃ O ₄	400	3	59	12	30
	250	21	88	0	12
	180	4	37	1	62
Pt/TiO ₂	400	16	73	21	6
	290	1	75	0	25
	180	1	84	0	16
	55	2	98	0	2

Reaction conditions: 20 mL of 0.5 M crotonaldehyde in 1,4-dioxane and 100 mg of freshly reduced Pt catalyst. Reaction temperature: 30°C ; initial hydrogen pressure: 0.414 MPa; reaction time, 8 h.

However, the strong peak at 116°C cannot be assigned to Pt species since, based on the calculated hydrogen uptake, the amount of Pt reduced was very high in relation to the nominal content of the catalyst (5 wt%, Table 1). Therefore, it must be related to the support and probably due to partial reduction of Fe(III) to Fe(II). Any Pt reduction process would be concealed by the previous peak or related to those at 184 and 271°C , which must be due to Pt species interacting to a variable extent with the support.

The temperature-programmed reduction profile for Pt/TiO_2 was quite flat and contained few reduction peaks the strongest of which appeared at quite a low temperature (51°C). There were, however, other, weaker peaks at higher temperatures (190, 301, 471 and 694°C). The peak at 51°C can be assigned to the reduction of PtO_x species to Pt^0 , and those at 471 and 694°C to the reduction of TiO_2 , favored by the presence of metal Pt particles [40].

The TPR profiles for the catalysts were used to select their respective reduction temperatures with a view to optimizing their performance in the hydrogenation of crotonaldehyde. A temperature of 400°C was used for all catalysts in addition to variable others signalling the presence of reduction peaks for Pt in the profiles. Table 2 shows the specific temperatures used to reduce each catalyst.

3.1.3. XRD diffraction

Fig. 2 shows the XRD patterns for the catalysts used in the hydrogenation of crotonaldehyde, which were reduced at the selected temperatures established from the TPR profiles. As can be seen, there were some general trends in the solids. Thus, the catalysts with a Fe-containing support (*viz.* $\text{Pt}/\text{Fe}_2\text{O}_3\text{-130}$ and $\text{Pt}/\text{Fe}_3\text{O}_4\text{-250}$) exhibited a strong, relatively sharp band in the region for Pt^0 ($2\theta = 46.7$), which suggests low dispersion of platinum and its presence as large particles relative to other catalysts. Solid $\text{Pt}/\text{TiO}_2\text{-400}$ exhibited a narrow, weaker band at $2\theta = 46.7$ the width at half height of which is also suggestive of low dispersion of Pt (*i.e.* particles of an increased size). Also, its lower strength is consistent with the results of the chemical elemental analysis (Table 1), which, based on the ICP-MS results and, especially, the EDX results, revealed that the catalyst was that containing the lowest propor-

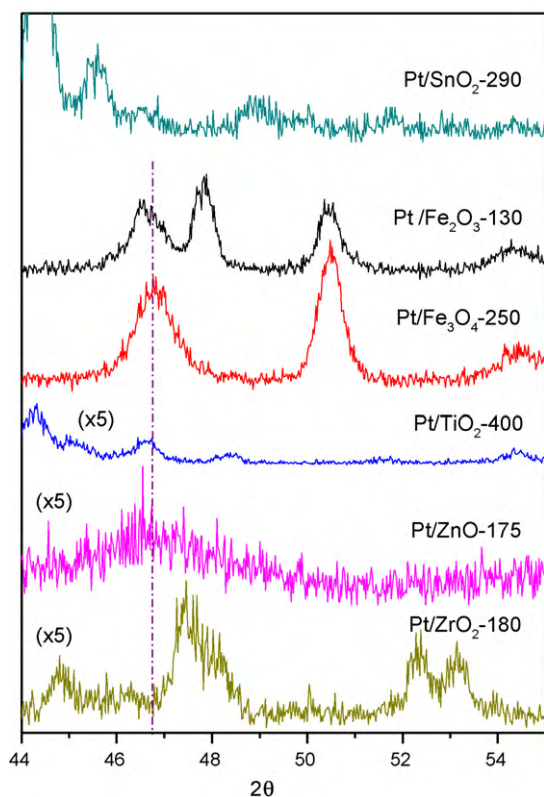


Fig. 2. X-ray diffraction patterns obtained for the Pt catalysts reduced at selected temperatures.

tion of Pt. Solid Pt/ZnO-175 exhibited a very broad band in the region for Pt⁰ suggesting high dispersion of Pt present as small metal particles. Pt/SnO₂-290 was special in that it exhibited a band at $2\theta = 48.9$ previously assigned to a Pt–Sn alloy and observed in catalysts reduced at temperatures as low as 170 °C [12]. Finally, solid Pt/ZrO₂-180 exhibited no band in the region for Pt⁰, possibly as a result of a low Pt content – inconsistent with the chemical analysis of the solid, Table 1 –, or more likely a high dispersion of the metal phase.

3.1.4. Transmission electron microscopy

Following reduction at their chosen temperatures, the studied catalysts were examined by transmission electron microscopy (TEM). Fig. 3 shows their micrographs, which support the results previously obtained from the XRD patterns. Thus, solids Pt/Fe₂O₃-130, Pt/Fe₃O₄-250 and Pt/TiO₂-400 exhibited large, round-shaped particles of Pt consistent with their low metal dispersion. On the other hand, Pt/ZnO-175 exhibited a highly uniform (monodisperse) distribution of small Pt particles on the support; again, the results are consistent with the XRD patterns for this catalyst, which exhibited a very broad band in the Pt⁰ region. This is the most salient feature in our catalysts and could provide crucial information about the catalytic process.

Solid Pt/ZnO-175 was additionally examined by HRTEM (Fig. 4), and so was Pt/ZnO-400 by TEM (Fig. 5) and XRD (Fig. 6). Fig. 4 testifies to the highly uniform, narrow distribution (2–3 nm) of metal particle size in Pt/ZnO-175. As can be seen from the micrographs of Fig. 5, raising the calcination temperature from 175 to 400 °C increased the size of metal particles very slightly. In fact, the mean size of Pt particles as determined by TEM was 2.5 nm (36% dispersion) for Pt/ZnO-175 and 3.5 nm (26% dispersion) for Pt/ZnO-400. However, the XRD patterns of Fig. 6 reveal a substantial change in metal species. Thus, solid Pt/ZnO-400 exhibited a broad band at

high 2θ values relative to Pt/ZnO-175, probably as a result of the formation of a PtZn alloy [16,35].

3.1.5. X-ray photoelectron spectroscopy

The nature and oxidation state of Pt species (Pt⁰, Pt²⁺ and Pt⁴⁺) are usually determined with the XPS technique and, specifically, from the Pt(4f) peak [41–44]. The binding energy of metal Pt for 4f_{7/2} electrons is known to be 70.7–70.9 eV and that for 4f_{5/2} electrons 74.0–74.2 eV. The oxidized states of platinum have much higher binding energies (viz. 72.8–73.1 eV for 4f_{7/2} electrons and 76.1–76.4 eV for 4f_{5/2} electrons in Pt²⁺, and 74.0–74.9 eV for 4f_{7/2} electrons and 77.3–78.2 eV for 4f_{5/2} electrons in Pt⁴⁺).

Fig. 7 shows the XPS profiles for Pt(4f) and Zn(2p) in the calcined solids, and in those activated at 175 and 400 °C. The calcined, unactivated solid exhibited signals for two different Pt species, namely: Pt²⁺ (maxima at 72.7 and 76.2 eV) and Pt⁴⁺ (maxima at 74.7 and 78.0 eV); the latter were due to PtO₂ (74.0 eV), PtCl₄ (75.1 eV) or, more probably, to some intermediate species (e.g. Pt oxychlorinated species) [45]. The XPS profile for the Zn solid exhibited several peaks including one at 1021.6 eV associated to Zn²⁺ in ZnO and another at 1022.4 eV associated to a more unshielded Zn²⁺ species than that in ZnO.

Reducing the solids at 175 °C altered their XPS profiles, which now contained signals for two different Pt species. One, Pt⁰, gave signals at 70.9 and 74.2 eV and another, Pt²⁺, which was also detected in the XPS profile for the unreduced catalyst, appeared at 72.1 and 75.4 eV. The profile for Zn(2p) was similar to that for the unactivated catalyst with a signal at 1022.4 eV potentially due to a highly electron-deficient surface species of the ZnO_xCl_y type around Pt particles and resembling that reported by Ammari et al. in exchloride Pt/ZnO catalysts [35], where chloride ions would come from the decomposition of Pt precursor species released during the Pt⁴⁺ → Pt²⁺ → Pt⁰ reduction process.

Finally, the dominant Pt species in the solid reduced at 400 °C was Pt⁰ (70.9 and 74.2 eV). There were, however, additional, a weak signal in the regions for Pt²⁺ (71.7 and 74.9 eV). The signal for Zn(2p) was similar to that for the catalyst reduced at 175 °C; thus, the band associated to ZnO_xCl_y species (1022.4 eV) decreased in proportion to the increase in the band associated to Zn²⁺ in ZnO (1021.6 eV); this suggests that Zn oxychloride species gradually disappear as the support is reduced at a high temperature.

3.2. Liquid-phase hydrogenation of crotonaldehyde

3.2.1. Influence of the support and the catalyst reduction temperature

The influence of the reduction temperature of the catalyst on its activity and selectivity in the liquid-phase hydrogenation of crotonaldehyde was studied by using various catalysts reduced at selected temperatures. Reduction temperature was chosen according to significant features observed in the temperature-programmed reduction profiles (Fig. 1). In any case, all catalysts were reduced at 400 °C in addition to such selected temperatures. Catalytic runs were conducted at 30 °C, using 1,4-dioxane as solvent. The activity and selectivity results thus obtained after 8 h reaction are summarized in Table 2.

Solid Pt/ZrO₂ exhibited the highest crotonaldehyde conversion irrespective of the reduction temperature (400, 317 and 180 °C). On the other hand, its selectivity towards the unsaturated alcohol was rather low (5–6%) at the three temperatures. In any case, it provided acceptable activity at low reduction temperatures.

Pt/ZnO was scarcely active in the hydrogenation of crotonaldehyde, with conversion values in the region of 1% irrespective of its reduction temperature. On the other hand, it exhibited a high selectivity towards the unsaturated alcohol (especially when reduced at 175 °C, with 75% selectivity for crotyl alcohol). Raising its reduction

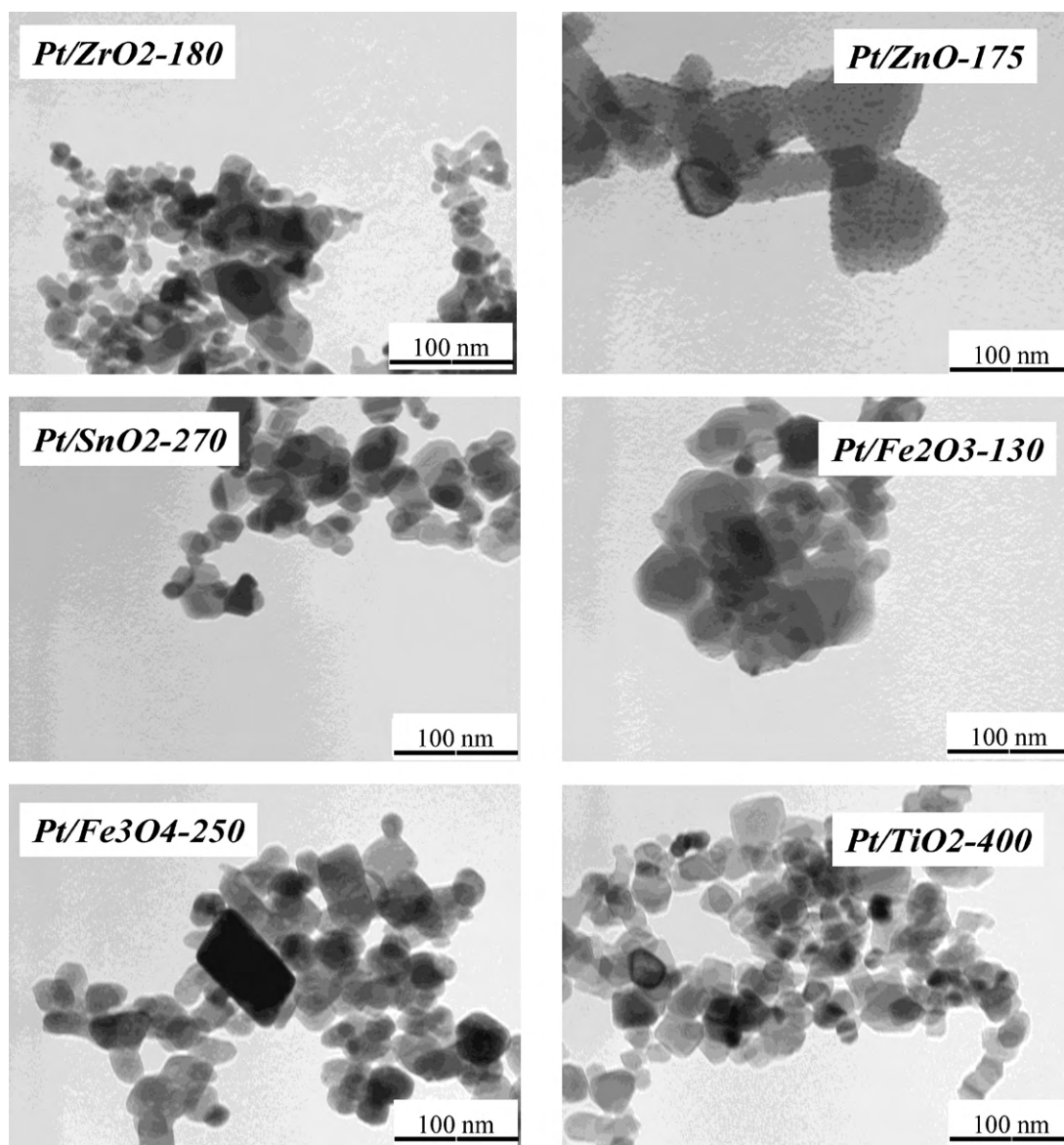


Fig. 3. Transmission electron microscopy images for the catalyst reduced at selected temperatures (magnification: 250k \times).

temperature considerably decreased its selectivity for the unsaturated alcohol (to 23%). In theory, the presence of a PtZn alloy detected in the XRD patterns for the solid reduced at 400 °C resulted in no increased selectivity towards the unsaturated alcohol relative to the solid reduced at 175 °C, which was found to contain no such alloy. These results contradict others previously obtained by Touroude et al. [16,35].

Catalyst Pt/SnO₂ exhibited rather poor conversion values whichever its reduction temperature (400, 290 or 190 °C). Although conversion increased slightly with increasing temperature, the increase was accompanied by a decrease in selectivity towards the unsaturated alcohol, which was only 4% for the solid reduced at 400 °C (with 3% conversion).

Among iron oxide-supported catalysts, Pt/Fe₂O₃ exhibited a dramatic loss of activity (2% conversion, 25% selectivity towards 2-butenol) in the solids reduced at high temperatures relative to that reduced 130 °C, which provided 20% conversion with 15% selectivity towards the alcohol. Solid Pt/Fe₃O₄ provided relatively poor conversion at both high (400 °C) and low (180 °C) reduction temperatures relative to its intermediate level (250 °C),

which exhibited 12% selectivity towards the unsaturated alcohol. The Pt/Fe₃O₄ catalyst reduced at 180 °C was the most suitable as regards selectivity for the alcohol, with 62% at 4% conversion.

Finally, as far as Pt/TiO₂ catalyst is concerned, results indicate that high reduction temperature (400 °C) lead to higher conversion as compared to the low temperature reduced solid, although associated to low crotyl alcohol selectivity.

The best overall catalytic performance was that of catalyst Pt/ZrO₂-400 ($X_{UAL} = 50\%$), which, however, exhibited the lowest selectivity towards crotyl alcohol ($S_{UOL} = 2\%$). The catalysts with an iron oxide support reduced at medium-low temperatures (*viz.* Pt/Fe₂O₃-130 and Pt/Fe₃O₄-250) had a moderate catalytic activity (about 20%) and a selectivity for crotyl alcohol of 12–15%. Finally, the best selectivity towards crotyl alcohol was provided by Pt/ZnO, especially when reduced at 175 °C; however, its favorable selectivity was accompanied by a very low conversion to crotonaldehyde ($X_{UAL} = 1\%$, $S_{UOL} = 75\%$). As stated before, Pt dispersion drastically changes from one catalyst to another and, as a result, activity and selectivity can also be affected. However, this influence cannot be

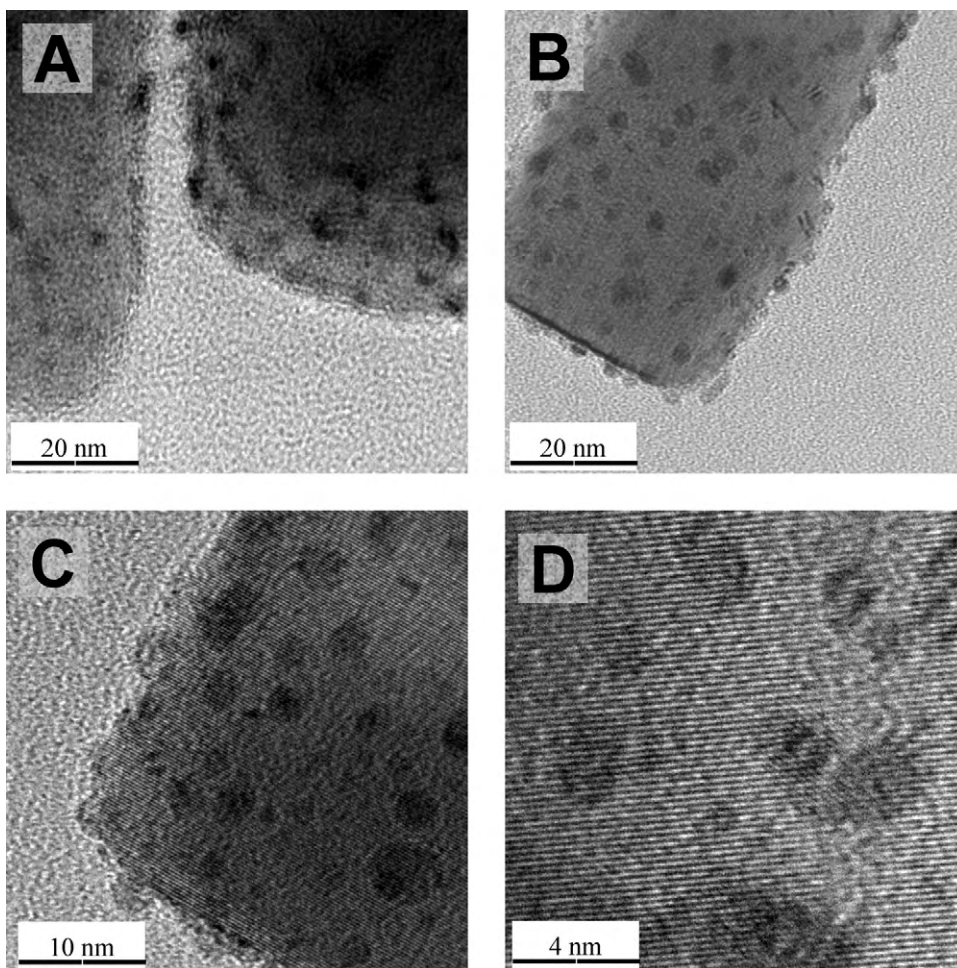


Fig. 4. High resolution transmission electron microscopy (HRTEM) images for the Pt/ZnO catalyst reduced at 175 °C (Pt/ZnO-175). (A) 250k \times ; (B) 250k \times ; (C) 500k \times ; (D) 1000k \times .

quantified due to differences in catalyst supports that clearly affect the overall behavior of the catalysts.

3.2.2. Influence of the solvent

After the initial screening of supports and reduction temperatures, we examined the influence of the solvent on the catalytic activity and selectivity of the solids on the liquid-phase hydrogenation of crotonaldehyde. The tests involved the supported catalysts obtained at the particular reduction temperature leading to the best activity and/or selectivity results. No alcohols were used as solvents in order to avoid the potential formation of hemiacetals and acetals from the carbonyl compounds [46]. Instead, the study was conducted in mixtures of 1,4-dioxane and water in variable ratios up to 1:1 that were supplied with moderate amounts of acetic acid or potassium hydroxide to adjust the pH to 3.5 and 13.0, respectively. The results thus obtained in the hydrogenation of crotonaldehyde are shown in Table 3.

1,4-Dioxane is a non-protic polar solvent highly miscible with water and possessing a low dielectric constant ($\epsilon_r = 2.21$), a relatively low dipole moment ($\mu = 1.5 \times 10^{30}$ C m) and a normalized empirical parameter for solvent polarity $E_T^N = 0.164$ on a scale ranging from 0 for tetramethylsilane to 1 for water [47,48]. The *donor number* (DN) is a measure of the Lewis basicity (*i.e.* the ability to donate an electron pair) in a solvent. 1,4-Dioxane has a DN^N value of 0.38 on a scale from 0 to 1, which suggests that it possesses donor properties due to unshared electrons in its oxygen atoms. On the other hand, the *acceptor number* (AN), that is, the ability to accept

an electron pair is rather low ($AN = 10.8$) [47]. Inasmuch as this is a non-protic solvent, it can form no hydrogen bonds by donating a hydrogen; however, it can readily form such bonds by having their unshared electrons accept a hydrogen atom. These properties can be quantified via parameters α (hydrogen donors) and β (hydrogen acceptors), which were introduced by Kamlet and Taft and listed in ref [47]. 1,4-Dioxane has $\alpha = 0.00$ and $\beta = 0.37$.

Water possesses a high dielectric constant ($\epsilon_r = 78.54$) and a greater dipole moment than 1,4-dioxane ($\mu = 6.2 \times 10^{30}$ C m). It is a highly polar solvent with $E_T^N = 1$ (the upper limit of the scale for the empirical polarity parameter). In addition, it has a donor number of 0.46, which is similar to that for 1,4-dioxane, but can accept electron pairs more readily (*i.e.* it is a better electron acceptor, with $AN = 54.8$) than this solvent. Finally, it has a much higher hydrogen donor capacity than 1,4-dioxane ($\alpha = 1.17$) in addition to a similar proton acceptor capacity ($\beta = 0.47$) [47,48].

Introducing water in the reaction medium had little effect on crotonaldehyde conversion or selectivity towards the unsaturated alcohol (Table 3, $S_{ENOL} = 4\text{--}6\%$) with catalyst Pt/ZrO₂-180. However, acidifying the medium reduced the catalyst activity and completely suppressed the selectivity towards the unsaturated alcohol. On the other hand, the addition of KOH had the opposite effect and raised the conversion to 47% and the selectivity towards 2-butenol to 10%.

For the Pt/ZnO-175 catalyst, the addition of water to the reaction medium had a strong effect on catalytic performance of the solid. Thus, it increased crotonaldehyde conversion to 11–13% with a selectivity towards the unsaturated alcohol in the 92–96% range.

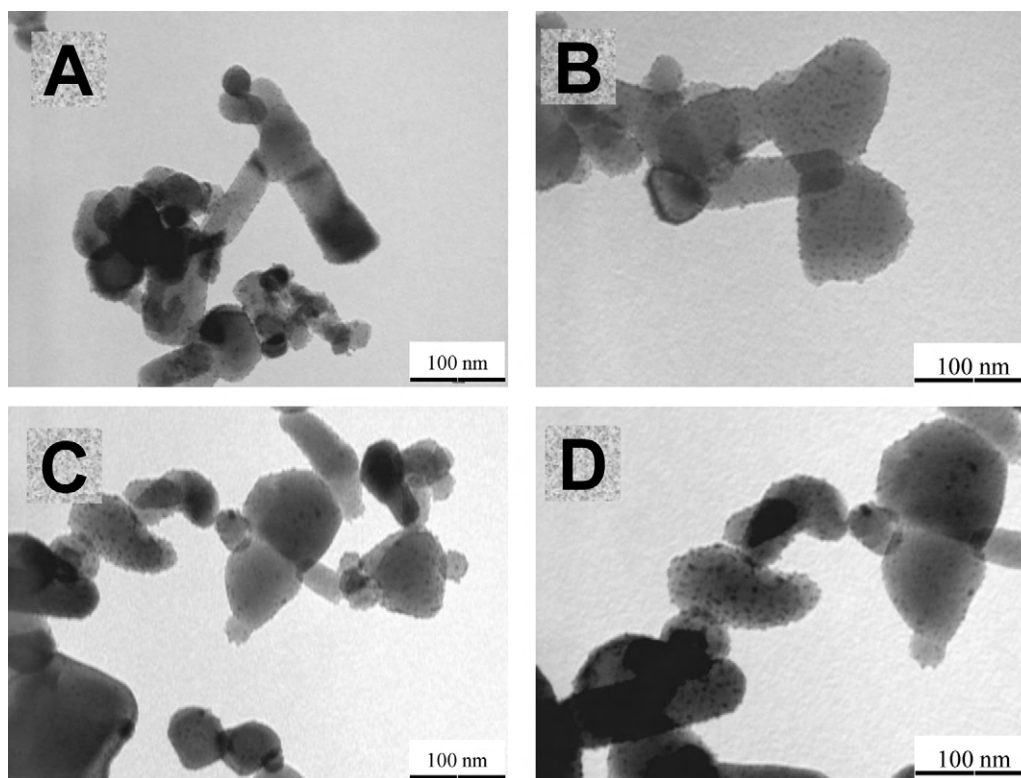


Fig. 5. Transmission electron microscopy images for the Pt/ZnO catalyst reduced at 400 °C (Pt/ZnO-400). (A) and (B) Pt/ZnO-175 at 250k \times ; (C) and (D) Pt/ZnO-400 at 250k \times .

However, adding an acid or base to the medium had no appreciable effect on the reaction, the mixture 1,4-dioxane/water providing the best results in any case.

Dioxane–water systems provided conversions similar to those obtained with pure dioxane with solid Pt/SnO₂-270; such conversions never exceeded 1%. Acidifying or alkalinizing the medium resulted in zero conversion of crotonaldehyde after 8 h reaction.

With the iron oxide-based catalysts (Pt/Fe₂O₃-130 and Pt/Fe₃O₄-250), adding water to the medium resulted in a very substantial loss of catalytic activity, which fell below 6% (against about 20% in pure dioxane). On the other hand, the presence of water raised the selectivity towards the unsaturated alcohol to 50–80%. The best overall performance as regards converting crotonaldehyde into 2-butenol (*viz.* 3% conversion and $S_{\text{ENOL}} = 81\%$) was that

Table 3

Solvent effect on the activity (crotonaldehyde conversion, X_{UAL}) and selectivity to butanal (S_{SAL}), 1-butanol (S_{SOL}) and crotyl alcohol (S_{UOL}) obtained in the liquid-phase crotonaldehyde hydrogenation.

Catalyst	Solvent	X_{UAL} (%)	S_{SAL} (%)	S_{SOL} (%)	S_{UOL} (%)
Pt/ZrO ₂ -180	1,4-Dioxane	37	82	14	4
	1,4-Dioxane/water	36	84	10	6
	1,4-Dioxane/water/H ⁺	13	94	6	0
	1,4-Dioxane/water/OH ⁻	47	83	7	10
Pt/ZnO-175	1,4-Dioxane	1	25	0	75
	1,4-Dioxane/water	11	5	0	96
	1,4-Dioxane/water/H ⁺	12	8	0	92
	1,4-Dioxane/water/OH ⁻	13	5	0	95
Pt/SnO ₂ -270	1,4-Dioxane	1	75	0	25
	1,4-Dioxane/water	1	44	0	56
Pt/Fe ₂ O ₃ -130	1,4-Dioxane	20	56	29	15
	1,4-Dioxane/water	3	19	0	81
	1,4-Dioxane/water/H ⁺	2	44	2	55
	1,4-Dioxane/water/OH ⁻	4	35	0	65
Pt/Fe ₃ O ₄ -250	1,4-Dioxane	21	88	0	12
	1,4-Dioxane/water	2	49	0	51
	1,4-Dioxane/water/H ⁺	1	40	0	60
	1,4-Dioxane/water/OH ⁻	6	30	0	70
Pt/TiO ₂ -400	1,4-Dioxane	16	73	21	6
	1,4-Dioxane/water	10	73	0	27
	1,4-Dioxane/water/H ⁺	69	88	5	7
	1,4-Dioxane/water/OH ⁻	15	83	7	11

Reaction conditions: 20 mL of 0.5 M crotonaldehyde and 100 mg of freshly reduced Pt catalyst. Reaction temperature: 30 °C; initial hydrogen pressure: 0.414 MPa; reaction time, 8 h.

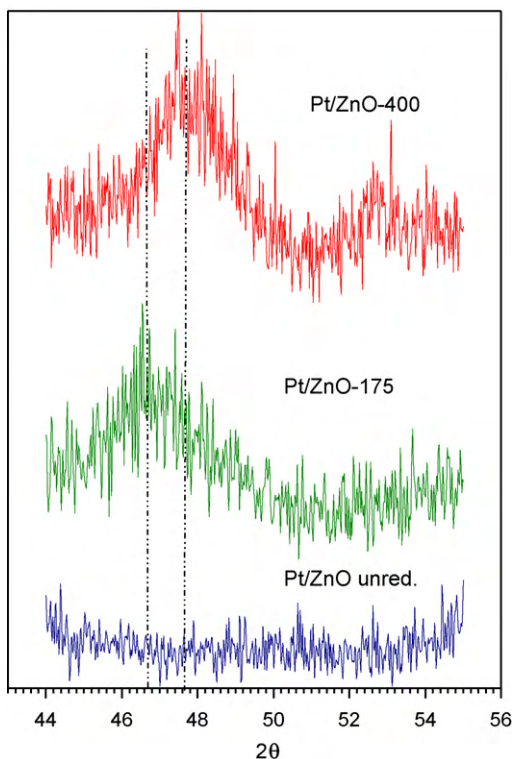


Fig. 6. X-ray diffraction patterns obtained for the unreduced Pt/ZnO and Pt/ZnO catalyst reduced at 175 and 400 °C.

obtained with Pt/Fe₂O₃-130 in a neutral 1,4-dioxane/water mixture as solvent. However, the iron-based support was found to exhibit signs of partial redissolution after 8 h reaction.

As with the previous solids, adding water to the 1,4-dioxane solvent was found to diminish the conversion obtained with

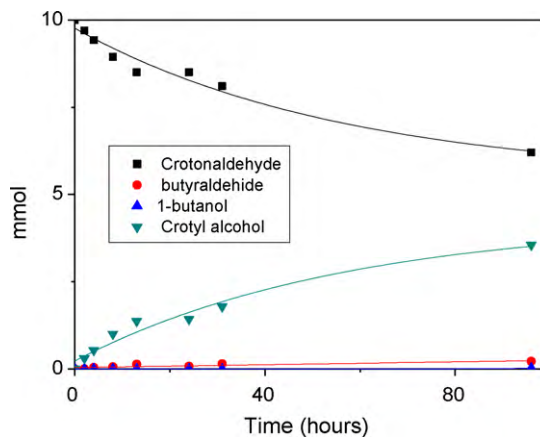


Fig. 8. Product distribution profile obtained in the liquid-phase selective hydrogenation of crotonaldehyde at the best reaction conditions: 100 mg of Pt/ZnO catalyst reduced at 175 °C (Pt/ZnO-175), water–dioxane (1:1) as solvent, 0.414 MPa of initial hydrogen pressure and a reaction temperature of 30 °C.

Pt/TiO₂-400 while raising its selectivity towards the unsaturated alcohol from 6 to 27%. Also, acidifying the medium caused a marked increase in molar conversion, which amounted to 69% after 8 h reaction—albeit, with a 2-butenol selectivity of only 7%.

In summary, the addition of water to the reaction medium tended to increase the yield in unsaturated alcohol, with the exception of solids Pt/Fe₂O₃-130 and Pt/Fe₃O₄-250. As noted earlier, however, the poor results for these two catalysts can be ascribed to the water added dissolving their supports. The favorable effect of water on the 2-butenol yield may have resulted from the water activating the carbonyl group by hydrogen bonding; in fact, the Kamlet–Taft parameter for water, $\alpha = 1.17$, is very high relative to 1,4-dioxane ($\alpha = 0.00$).

More specifically, the addition of KOH to the reaction medium (a dioxane/water mixture) provided the best yields in 2-butenol

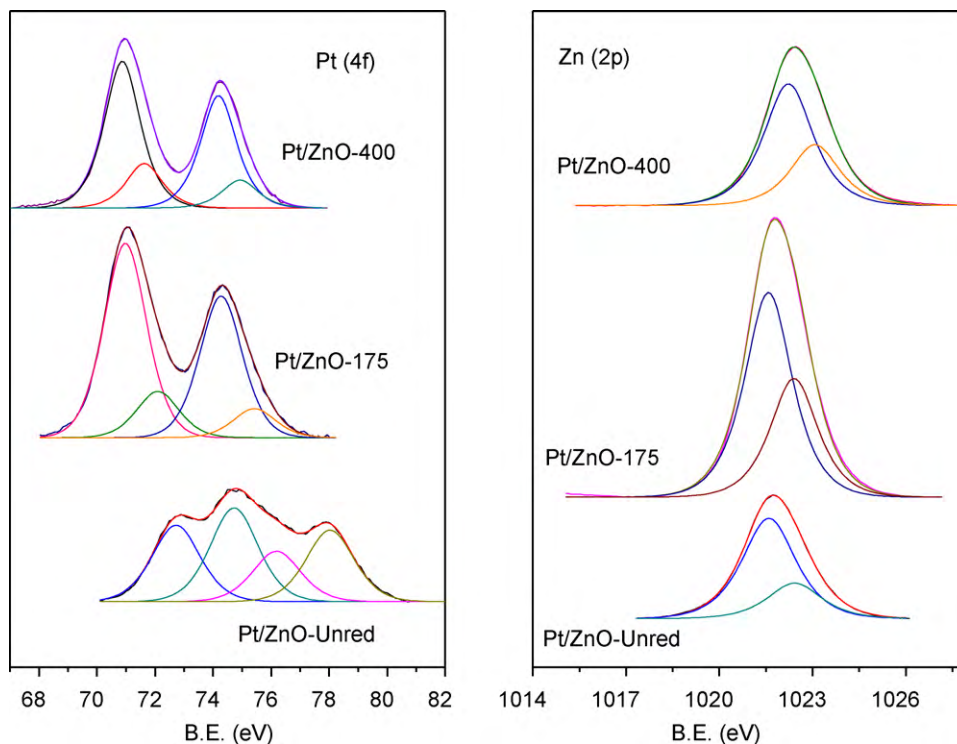


Fig. 7. XPS profiles in the Pt(4f) and Zn(2p) region obtained for the unreduced Pt/ZnO and Pt/ZnO catalyst reduced at 175 and 400 °C.

with solids Pt/ZrO₂-180 and Pt/ZnO-175. Only Pt/TiO₂-400 provided high yields with an acid medium, however. In any case, the gains obtained by adding KOH cannot offset the environmental hazard associated with the use of an alkaline medium.

3.2.3. Product distribution profile under the optimum conditions

The best reaction conditions were taken to be those leading to the highest yield in the unsaturated alcohol (2-butenol). Based on the above-discussed results, Pt/ZnO-175 was the solid providing the best yield in a medium consisting of a dioxane/water mixture, whether acid, neutral or alkaline. In any case, the presence of an alkali resulted in little improvement, so its addition to the reaction medium was unwarranted. For this catalyst and reaction conditions the turnover obtained (Pt/ZnO-175, TOF = $4 \times 10^{-3} \text{ s}^{-1}$) is lower by a factor of 10 than those described by Bartok et al. [28] for some commercial and clay-supported Pt catalyst in the liquid-phase crotonaldehyde hydrogenation. However the selectivity to crotyl alcohol achieved with our catalyst ($S_{\text{UOL}} = 96\%$ at 11% conversion, 91% at 40% conversion) is largely higher than those reported in that work ($S_{\text{UOL}} = 7\text{--}43\%$). This high selectivity of solid Pt/ZnO-175 may have resulted from the presence of ZnO_xCl_y formed around Pt particles and detected in the XPS analysis which might have acted as Lewis acid sites facilitating anchoring of the crotonaldehyde molecule via its carbonyl double bond [35]. On the other hand, the PtZn alloy detected in the solid reduced at 400 °C seemingly had no clear-cut effect on the selectivity of the process. For the Pt/ZnO-400 catalyst, at best reaction conditions, the turnover was TOF = $2.5 \times 10^{-3} \text{ s}^{-1}$ similar than that achieved for the catalyst reduced at 175 °C (TOF = $4 \times 10^{-3} \text{ s}^{-1}$). Moreover, as far as the selectivity to crotyl alcohol is concerned, it was also in the level of the Pt/ZnO-175 catalyst ($S_{\text{UOL}} = 95\%$ at 5% conversion). Therefore, in this case no structure sensitivity was apparently observed, probably due to the small change in Pt particle size, or to the additional effect of the PtZn alloy formed at high reduction temperature.

Fig. 8 shows the product distribution profile for solid Pt/ZnO-175 in a medium consisting of 1:1 dioxane/water. As can be seen, crotonaldehyde conversion increased gradually with conversion close to 40% and no signs of catalyst deactivation after 96 h reaction. The selectivity towards 2-butenol was very high (91–96%) throughout the selective hydrogenation of crotonaldehyde. This is an excellent selectivity and a more than acceptable conversion level that is very difficult to obtain under so mild reaction conditions (at reaction temperature of 30 °C and an initial hydrogen pressure of 0.414 MPa) with a platinum catalyst.

4. Conclusions

The selective reduction of crotonaldehyde to crotyl alcohol over Pt catalysts supported on various partially reducible solids including Fe₂O₃, Fe₃O₄, ZrO₂, ZnO, TiO₂ and SnO₂ was conducted. The catalysts were characterized by thermal programmed reduction (TPR) and reduced at temperatures that were selected as a function of the presence of specific reduction peaks for Pt in the TPR profiles. The use of low reduction temperatures was found to provide catalysts leading to increased yields in the unsaturated alcohol (2-butenol) in the selective hydrogenation of crotonaldehyde. The high selectivity of solid Pt/ZnO-175 may be related to the presence of ZnO_xCl_y species forming around Pt particles and detected by XPS which might act as Lewis acid sites facilitating anchoring of the crotonaldehyde molecule via its carbonyl double bond [35]. On the other hand, the PtZn alloy detected in the solid reduced at 400 °C has no clear-cut effect on the selectivity of the process.

As regards the influence of the reaction medium in general and the addition of water to a neutral, acid or alkaline medium in particular, the latter was found to raise the yield in unsaturated alcohol,

especially if the medium was alkalinized with KOH. However, the resulting improvement cannot offset the disadvantage of requiring the use of additives increasing the complexity of the reaction medium and detracting from environmental friendliness.

The best operating conditions as regards 2-butenol yield were used to determine the product distribution profile, using a dioxane/water mixture as solvent and solid Pt/ZnO-175 as catalyst. Based on the profile, crotonaldehyde conversion increased gradually with time; also, conversion was close to 40% and the catalyst exhibited no signs of deactivation after 96 h reaction. In addition, the selectivity towards 2-butenol was very high (91–96%) throughout the selective reduction of crotonaldehyde. This selectivity level is excellent and the conversion level quite acceptable and very difficult to obtain with platinum catalysts under such mild conditions (a reaction temperature of 30 °C and an initial hydrogen pressure of 0.414 MPa).

Acknowledgements

This research was funded by Spain's Ministry of Science and Education (Projects CTQ2008-01330/BQU and CTQ2007-65754/PPQ), and cofunded by FEDER and the Andalusian Regional Government (Projects P07-FQM-02695 and P09-FQM-4781).

References

- [1] B. Chen, U. Dingerdissen, J.G.E. Krauter, H.G.J. Lansink Rotgerink, K. Mobus, D.J. Ostgard, P. Panster, T.H. Riermeier, S. Seebald, T. Tacke, H. Trauthwein, *Appl. Catal. A* 280 (2005) 17–46.
- [2] P. Maki-Arvela, J. Hajek, T. Salmi, D.Y. Murzin, *Appl. Catal. A* 292 (2005) 1–49.
- [3] P. Gallezot, D. Richard, *Catal. Rev. -Sci. Eng.* 40 (1998) 81–126.
- [4] P. Gallezot, P.J. Cerino, B. Blanc, G. Fleche, P. Fuertes, *J. Catal.* 146 (1994) 93–102.
- [5] N. Mahata, F. Goncalves, M.F. Pereira, J.L. Figueiredo, *Appl. Catal. A* 339 (2008) 159–168.
- [6] N.M. Bertero, A.F. Trasarti, B. Moraweck, A. Borgna, A.J. Marchi, *Appl. Catal. A* 358 (2009) 32–41.
- [7] F. Coloma, J. Llorca, N. Homs, P. Ramirez de la Piscina, F. Rodriguez-Reinoso, A. Sepulveda-Escribano, *Phys. Chem. Chem. Phys.* 2 (2000) 3063–3069.
- [8] G. Szollosi, B. Torok, L. Baranyi, M. Bartok, *J. Catal.* 179 (1998) 619–623.
- [9] Z.M. Michalska, B. Ostaszewski, J. Zientarska, J.M. Rynkowski, *J. Mol. Catal. A* 185 (2002) 279–283.
- [10] C. Milone, R. Ingoglia, L. Schipilliti, C. Crisafulli, G. Neri, S. Galvagno, *J. Catal.* 236 (2005) 80–90.
- [11] A. Dandekar, M.A. Vannice, *J. Catal.* 183 (1999) 344–354.
- [12] K. Liberikova, R. Touroude, D.Y. Murzin, *Chem. Eng. Sci.* 57 (2002) 2519–2529.
- [13] H. Yoshitake, Y. Iwasawa, *J. Catal.* 125 (1990) 227–242.
- [14] H. Yoshitake, Y. Iwasawa, *JCS, Faraday Trans.* 88 (1992) 503–510.
- [15] X. Han, R. Zhou, B. Yue, X. Zheng, *Catal. Lett.* 109 (2006) 157–161.
- [16] M. Consonni, D. Jolic, D. Yu Murzin, R. Touroude, *J. Catal.* 188 (1999) 165–175.
- [17] S. Bernal, J.J. Calvino, M.A. Cauqui, J.M. Gatica, C. Lopez Cartes, J.A. Perez Omil, J.M. Pintado, *Catal. Today* 77 (2003) 385–406.
- [18] M. Abid, G. Ehret, R. Touroude, *Appl. Catal. A* 217 (2001) 219–229.
- [19] M. Abid, V. Paul-Boncour, R. Touroude, *Appl. Catal. A* 297 (2006) 48–59.
- [20] A. Sepulveda-Escribano, F. Coloma, F. Rodriguez-Reinoso, *J. Catal.* 178 (1998) 649–657.
- [21] P. Concepcion, A. Corma, J. Silvestre-Albero, V. Franco, J.Y. Chane-Ching, *J. Am. Chem. Soc.* 126 (2004) 5523–5532.
- [22] H.G. Manyar, D. Weber, H. Daly, J.M. Thompson, D.W. Rooney, L.F. Gladden, E. Hugh Stitt, J. Jose Delgado, S. Bernal, C. Hardacre, *J. Catal.* 265 (2009) 80–88.
- [23] U.K. Singh, M.A. Vannice, *Appl. Catal. A* 213 (2001) 1–24.
- [24] S. Mukherjee, M.A. Vannice, *J. Catal.* 243 (2006) 108–130.
- [25] S. Mukherjee, M.A. Vannice, *J. Catal.* 243 (2006) 131–148.
- [26] M. Englisch, A. Jentys, J.A. Lercher, *J. Catal.* 166 (1997) 25–35.
- [27] M.A. Aramendia, V. Borau, C. Jimenez, J.M. Marinas, A. Porras, F.J. Urbano, *J. Catal.* 172 (1997) 46–54.
- [28] I. Kun, G. Szollosi, M. Bartok, *J. Mol. Catal. A* 169 (2001) 235–246.
- [29] H. Yamada, S. Goto, *J. Chem. Eng. Jpn.* 36 (2003) 586–589.
- [30] S.I. Fujita, Y. Sano, B.M. Bhanage, M. Arai, *J. Catal.* 225 (2004) 95–104.
- [31] E. Gebauer-Henke, J. Grams, E. Szubiakiewicz, J. Farbotko, R. Touroude, J. Rynkowski, *J. Catal.* 250 (2007) 195–208.
- [32] D.L. Hoang, H. Lieske, *Catal. Lett.* 27 (1994) 33–42.
- [33] J.M. Moreno, M.A. Aramendia, A. Marinas, J.M. Marinas, F.J. Urbano, *Appl. Catal. B* 59 (2005) 275–283.
- [34] T. Mitsui, K. Tsutsui, T. Matsui, R. Kikuchi, K. Eguchi, *Appl. Catal. B* 78 (2008) 158–165.
- [35] F. Ammari, J. Lamotte, R. Touroude, *J. Catal.* 221 (2004) 32–42.
- [36] X. Wang, Y.C. Xie, *Catal. Lett.* 75 (2001) 73–80.

- [37] N. Apostolescu, B. Geiger, K. Hizbullah, M.T. Jan, S. Kureti, D. Reichert, F. Schott, W. Weisweiler, *Appl. Catal. B* 62 (2006) 104–114.
- [38] A. Venugopal, M.S. Scurrill, *Appl. Catal. A* 258 (2004) 241–249.
- [39] G. Munteanu, L. Ilieva, D. Andreeva, *Thermochim. Acta* 291 (1997) 171–177.
- [40] M.A. Aramendia, J.C. Colmenares, A. Marinas, J.M. Marinas, J.M. Moreno, J.A. Navio, F.J. Urbano, *Catal. Today* 128 (2007) 235–244.
- [41] T. Teranishi, M. Hosoe, T. Tanaka, M. Miyake, *J. Phys. Chem. B* 103 (1999) 3818–3827.
- [42] Y. Nagai, H. Shinjoh, K. Yokota, *Appl. Catal. B* 39 (2002) 149–155.
- [43] V. Romanovskaya, M. Ivanovskaya, P. Bogdanov, *Sens. Actuators, B* 56 (1999) 31–36.
- [44] S. Zafeiratos, G. Papakonstantinou, M.M. Jacksic, S.G. Neophytides, *J. Catal.* 232 (2005) 127–136.
- [45] C.D. Wagner, W.M. Riggs, L.E. Davis, J.F. Moulder, G.E. Muilenberg, *Handbook of X-Ray Photoelectron Spectroscopy. A Reference Book of Standard Data for Use in X-Ray Photoelectron Spectroscopy*, Perkin-Elmer Corporation, Minnesota, 1979.
- [46] J. Hajek, N. Kumar, P. Maki-Arvela, T. Salmi, D.Y. Murzin, I. Paseka, T. Heikkila, E. Laine, P. Laukkanen, J. Vayrynen, *Appl. Catal. A* 251 (2003) 385–396.
- [47] D.J. Adams, P.J. Dyson, S.T. Tavener, *Chemistry in Alternative Media*, John Wiley & Sons, Chichester, 2004.
- [48] C. Reichardt, *Solvents and Solvent Effects in Organic Chemistry*, 3rd ed., Wiley-VCH, Weinheim, 2003.